Eur Biophys J (2002) 31: 232–240
DOI 10.1007/s00249-002-0205-7

BIOPHYSICS LETTER

Milton Roque Bugs · Marinônio Lopes Cornélio

A new biophysics approach using photoacoustic spectroscopy to study the DNA-ethidium bromide interaction

Received: 9 August 2001 / Revised: 15 October 2001 / Accepted: 22 October 2001 / Published online: 14 February 2002
© EBSA 2002

Abstract We have examined the binding processes of ethidium bromide interacting with calf thymus DNA using photoacoustic spectroscopy. These binding processes are generally investigated by a combination of absorption or fluorescence spectroscopies with hydrodynamic techniques. The employment of photoacoustic spectroscopy for the DNA-ethidium bromide system identified two binding manners for the dye. The presence of two isosbestic points (522 and 498 nm) during DNA titration was evidence of these binding modes. Analysis of the photoacoustic amplitude signal data was performed using the McGhee-von Hippel excluded site model. The binding constant obtained was 3.4×10^{8} $M(bp)^{-1}$, and the number of base pairs excluded to another dye molecule by each bound dye molecule (n) was 2. A DNA drug dissociation process was applied using sodium dodecyl sulfate to elucidate the existence of a second and weaker binding mode. The dissociation constant determined was 0.43 mM, whose inverse value was less than the previously obtained binding constant, demonstrating the existence of the weaker binding mode. The calculated binding constant was adjusted by considering the dissociation constant and its new value was 1.2×10^{9} $M(bp)^{-1}$ and the number of excluded sites was 2.6. Using the photoacoustic technique it is also possible to obtain results regarding the dependence of the quantum yield of the dye on its binding mode. While intercalated between two adjacent base pairs the quantum yield found was 0.87 and when associated with an external site it was 0.04. These results reinforce the presence of these two binding processes and show that photoacoustic spectroscopy is more extensive than commonly applied spectroscopies.

M.R. Bugs · M.L. Cornélio (✉)
Departamento de Física, IBILCE,
Universidade Estadual Paulista (UNESP),
Rua Cristovão Colombo 2265, São José do Rio Preto,
São Paulo CEP 15054-000, Brazil
E-mail: mario@df.ibilce.unesp.br
Tel.: +55-17-2212246
Fax: +55-17-2212247

Keywords Photoacoustic spectroscopy · DNA · Ethidium bromide · Binding modes · Dissociation constant

Introduction

Ethidium bromide (Eb) is a powerful and versatile probe for studying the internal and external binding modes of dyes to nucleic acids. The mechanism most frequently associated with the binding of planar molecules is intercalation, the insertion of the planar portion of the molecule between the DNA base pairs (Lerman 1961; Waring 1965; LePecq and Paoletti 1967; Burns 1969; Douthart et al. 1973; Tsai et al. 1977; Bresloff and Crothers 1981). Eb is a polycyclic dye which obeys such interaction and the binding properties of intercalating have been associated with biological processes (McCann et al. 1975; Waring 1981). Intercalation has been shown to be the primary and generally stronger binding mode. While the second mode of site binding is thought to be an association between the dye molecules and an external site of DNA, a territorial binding in which the Eb interacts with DNA is dominated by Coulomb forces along the phosphate backbone, i.e., they move freely in a volume around the DNA (LePecq and Paoletti 1967; Nordmeier 1992; Yguerabide and Ceballos 1995).

Intercalation as the primary binding mode is observed by absorption spectroscopy supported by a red spectrum shift, a hypochromic effect relative to the free Eb spectrum. In fluorescence this event is detected because of the enhancement of the fluorescence amplitude after intercalation. However, the employment of these two techniques alone is not able to distinguish the second binding mode. The work of Nordmeier (1992) suggests and uses the absorption method combined with hydrodynamic techniques to determine the two binding modes and quantify the population of the Eb intercalated between and associated with DNA.

Photoacoustic spectroscopy (PAS) is presented here as a new approach to the study of the interaction

between drugs and DNA. This technique is different from the conventional techniques, although the incident energy is in the form of optical photons. The interaction of these photons with the sample under investigation is studied not through subsequent detection and analysis of some of the photons, but rather through a direct measure of the energy absorbed by the sample as a result of its interaction with the photon beam. The sample is illuminated with monochromatic light and if any of the incident photons are absorbed by the sample, internal energy levels within the sample are excited. Upon subsequent relaxation of these energy levels, all or part of the absorbed photon energy is then transformed into heat energy through nonradiative relaxation processes. So PAS is much more than conventional spectroscopy. It is, after all, a photocalorimetric method that measures how much of the electromagnetic radiation absorbed by a sample is actually converted into heat. As such, it can be used to measure the absorption or excitation spectrum, the lifetime of excited states, and the energy yield of radiative processes.

PAS has a wide application in the study of biological events such as photosynthesis (Malkin and Cahen 1979; Fork and Herbert 1993), electron transfer (Cornélio and Sanches 1994, 1995), protein analysis (Kurian et al. 1997), and protein folding (Abbruzzetti et al. 2000), as well as in the determination of quantum yield (Adams et al. 1977, 1980; Lahmann and Ludewig 1977; Quimby and Yen 1980; Mandelis 1982).

In recent work, we have investigated the nonradiative relaxation processes of Eb complexes with DNA, where we describe photoacoustic measurements of Eb triplet excited-state lifetimes at different ionic strengths, obtaining information about the molecular motion of DNA induced by salt, which are correlated with the FTIR measurements that identified the action of the counterion on the structure of DNA (Bugs 2001; Bugs and Cornélio 2001). This present paper is an extension of our studies with Eb and DNA, in which we have used the same photoacoustic spectrometer.

The objective of this paper, which concerns the use of a spectroscopic method that is not commonly applied to biophysical problems to determine binding modes, is to demonstrate the feasibility of PAS in detecting the two binding modes of Eb to DNA and to quantify the fractions of intercalated and outside bound dye molecules.

Materials and methods

Sample preparation

Ethidium bromide and NaBr (Sigma-Aldrich), sonicated calf thymus DNA (phenol extracted) and sodium dodecyl sulfate (SDS) (Amersham Pharmacia Biotech) were used without further purification. Doubly distilled water was used. A stock solution of Eb was prepared at 6 mM and DNA at 20 mM, both in 20 mM Tris-HCl buffer at pH 7.0 with 150 mM NaBr. The molar extinction coefficients of 5700 M^{-1} cm^{-1} at 480 nm and of 12,850 $M(bp)^{-1}$ cm^{-1} at 260 nm were used to determine the concentrations of Eb and DNA, respectively, in UV-visible absorption spectroscopy. For equilibrium binding titrations, the Eb concentration was kept at 2 mM and DNA varied from 0 to 11.06 mM, with a DNA:Eb molar ratio range from 0 to 5.53. The titrations of SDS varied from 0 to 30.98 mM. The PAS experiments were repeated in triplicate, with reproduction of the data. The sample liquid volume was kept at 200 μL, with concentration correction at each addition. The amount of DNA added to an Eb solution was performed with microliter syringes (Hamilton) in order to ensure the precise concentration and volume of the sample. All measurements were performed at 25 °C.

Photoacoustic measurements and analysis

The photoacoustic (PA) spectrometer uses a closed cylindrical cell with a microphone detector; it was constructed in our laboratory and the details of this have been previously presented (Bugs 2001; Bugs and Cornélio 2001). A 300 W xenon arc lamp was employed and focused at the entrance slit of the monochromator and a single beam was modulated by a mechanical chopper at 10 Hz. The cell was built of steel with a quartz window. The volume of the gas in the cell is 1 cm^3. The thickness of the sample is 2 mm when the cell contains 200 μL of liquid sample. Normalization of the spectra was achieved by using the PA spectrum of black carbon.

The pressure increase inside the PA cell is due to the surface temperature oscillations of the sample, which follows light absorption. The PA amplitude signal is proportional to the amount of light absorbed, which depends on the optical absorption coefficient $\beta = 2.303\varepsilon C$, where ϵ is the molar extinction coefficient and C is the concentration (Perkampus 1992). Therefore the PA spectrum lineshape is similar to that obtained from the absorption spectrum. Nevertheless, the PA amplitude signal also represents the amount of energy absorbed which was converted into heat, through the nonradiative relaxation process. It is clear that PA is a combination of optical spectroscopy and calorimetry, both obtaining the amount of heat produced and, as a complement of the radiative relaxation process, the quantum yield efficiency (Rosencwaig 1980).

Equilibrium binding constant

This technique has been successfully employed in DNA-dye binding studies. Essentially, a dye solution of fixed concentration is transferred to a sample holder and the progressive signal amplitude changes are recorded after addition of serial aliquots of a DNA solution. Optical and nonradiative deexcitation process changes are analyzed for the dye component alone in terms of the free dye and the resulting complex.

In the commonly applied methods the addition of the DNA solution to the dye solution results in a drop in absorbance and a fluorescence change that depends on the optical behavior of the dye being examined. Thus, a nonfluorescent dye forming a fluorescent complex will cause a fluorescence increase upon binding (LePecq and Paoletti 1967), whereas a PA response will cause an amplitude signal decrease (see Fig. 1).

Data analysis will be outlined for PA amplitude signal changes whose mathematical treatments are analogous to those of Jenkins (1997). The PA amplitude signal A_{PAS}, measured from 370 to 570 nm, reflects both the free Eb and DNA-Eb species:

$$A_{PAS} = A_{PAS_f} + A_{PAS_b} = \varepsilon_f C_f + \varepsilon_b C_b \quad (1)$$

where A_{PAS_f} is the free Eb and A_{PAS_b} is the Eb bound to DNA, and the fixed Eb concentration is $C = C_f + C_b$, where C_f is the concentration of free Eb and C_b is the concentration of Eb bound to DNA, and ϵ_f and ϵ_b represent the respective extinction coefficients. Binding analysis requires a determination of C_f, and hence the amount r of Eb bound per unit of DNA as a function of added DNA titrant.

Determination of C_f and r values during the titration is related to the Eb binding fraction α, and the equilibrium distribution at each titration position is calculated from:

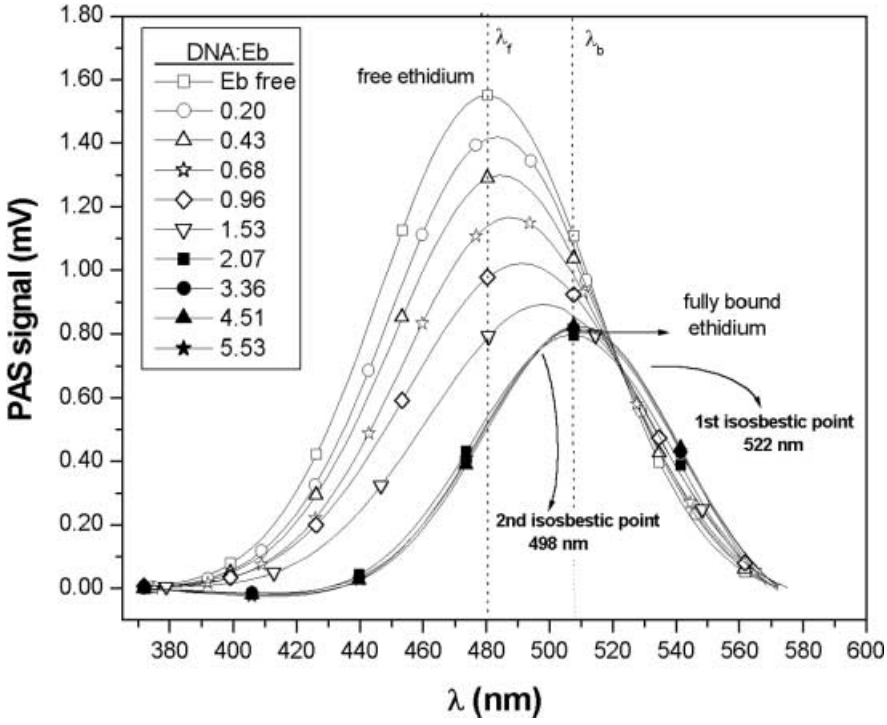

Fig. 1 Photoacoustic spectra of DNA titration to ethidium bromide with a concentration of 2.0 mM at 150 mM NaBr; the DNA:Eb molar ratio varied from 0 to 5.53. λ_f represents the maximum wavelength of free Eb in solution, and λ_b represents the Eb fully bound to DNA

$$\alpha = \frac{C_b}{C} = \frac{C - C_f}{C} = \frac{A_{PAS} - A_{PAS_f}}{A_{PAS_b} - A_{PAS_f}} \quad (2)$$

where A_{PAS_f} and A_{PAS_b} are the measured PA signals for the free and bound Eb to DNA, and A_{PAS} represents the amplitude of the PA signal at each titration. The fraction α varies on a 0 to 1 scale, while A_{PAS} varies from A_{PAS_f} to A_{PAS_b}. Then, $r = \alpha C/C_{DNA}$ and $C_f = (1-\alpha)C$, where C_{DNA} is the total concentration of DNA titrant at that point.

Binding analysis of the experimental r and C_f data has received much attention, and the treatment employed depends on the model used. For a simple two-state binding mode, the data can be fitted to the Scatchard equation by plotting r/C_f versus r. However, such a linear relationship is rare for a nucleic acid system and it is more usual to use the excluded site (neighbor exclusion) model developed by McGhee and von Hippel (1974) to consider occupancy of multiple binding sites:

$$r/C_f = K(1 - nr)[(1 - nr)/(1 - (n-1)r)]^{n-1} \quad (3)$$

where K is the binding constant to an isolated site and n is the neighbor exclusion parameter, i.e., the number of base pairs of DNA excluded by the bound Eb.

Dissociation constant

To determine the Eb concentration dissociated from DNA induced by SDS, we consider that DNA has two different kinds of site for the dye, which correspond to the model of nonequivalent sites binding (van Holde et al. 1998). To investigate the behavior of such systems, let us consider a simple case in which there are only two classes of sites: n_1 are strong sites and n_2 are weak sites, each with a microscopic association constant k_1 and k_2. Unless $k_1 \gg k_2$, it is very difficult to distinguish this situation from the binding by $(n_1 + n_2)$ equivalent sites, with k intermediate between k_1 and k_2, and the initial binding will be dominated by k_1. In our case the dissociation constant will be related to the second microscopic association constant k_2, which is the weak class of sites.

The Eb dissociation fraction α_d is analogous to Eq. (2) but with some modification because it now represents the amount of dye removed from DNA, written as:

$$\alpha_d = \frac{A_{PAS} - A_{PAS_b}}{A^*_{PAS_f} - A_{PAS_b}} \quad (4)$$

where $A^*_{PAS_f}$ and A_{PAS_b} are the PA amplitude signals for the removed and intercalated dye of the DNA-Eb complex. The $A^*_{PAS_f}$ describes the amount of dye removed from the DNA being captured by the SDS. The fraction α_d varies on a 0 to 1 scale, while A_{PAS} varies from A_{PAS_b} to $A^*_{PAS_f}$. The analysis of the dissociation process using the experimental α_d data is performed by fitting a rectangular hyperbola to the plot of α_d versus SDS concentration, obtaining the dissociation constant.

Results and discussion

We conducted the experiments in which the Eb equilibrium binding titration process to DNA was measured. The buffer used simulates the physiological condition. According to the literature, Eb binds to DNA by intercalation between two adjacent base pairs and there is also a certain suspicion about an external site, most likely along the phosphate backbone (LePecq and Paoletti 1967; Douthart et al. 1973; Yguerabide and Ceballos 1995). Recent studies (Nordmeier 1992; Heller and Greenstock 1994; Byrne and de Mello 1998) suggest the existence of two types of Eb binding to DNA, which depend directly on the saturation of Eb in the solution. The interaction of the DNA-Eb complex is usually investigated by absorbance or fluorescence techniques. When Eb forms a complex with DNA the electronic distribution of the ligand changes, which is perceptible in the absorbance spectrum with a simultaneous shift

to longer wavelength (bathochromic shift) and the decrement value of the molar extinction coefficient ϵ_{max} at the λ_{max} (hypochromic effect) (Jenkins 1997), whereas in fluorescence the signal amplitude increases after the formation of the DNA-Eb complex (LePecq and Paoletti 1967). These results were helpful in elucidating the mechanism of other drugs which interact with DNA. However, using these techniques alone it is not possible to confirm the manner in which the drug binds to DNA, whether by intercalation, groove binding, or external drug association, because all three can induce qualitatively similar effects (Li and Crothers 1969). The only reliable means to distinguish the binding process involves hydrodynamic methods (Nordmeier 1992; Suh and Chaires 1995). Nevertheless, in this study we have used PAS, which has proved to be an efficient tool, capable of distinguishing these two binding modes (Bugs 2001).

Essentially, an Eb solution of fixed concentration at 2.0 mM with 150 mM of NaBr was placed in a PA sample holder and the PA amplitude signal was recorded after each addition of aliquots of DNA solution at the same salt concentration. The results presented in Fig. 1 show the DNA titration to Eb, with the DNA:Eb molar ratio varying from 0 to 5.53. The evidence of Eb intercalated to DNA is observed because of a bathochromic shift of nearly 28 nm in the 480 nm absorption band, and also because of a hypochromic effect of 48.5% from the λ_{max} values. Besides that, it is possible to observe the existence of two isosbestic points, one at 522 nm with $\epsilon_{522} = 2560\ M^{-1}\,cm^{-1}$, and another at 498 nm with $\epsilon_{498} = 2800\ M^{-1}\,cm^{-1}$. These two points suggest two distinct binding equilibrium processes. During titration the first isosbestic point appeared at the molar ratio interval from 0 to 2.07, indicating the first binding equilibrium process. The second isosbestic point only appeared at the molar ratio interval from 2.07 to 5.53, indicating the existence of a second binding equilibrium process. So, these two distinct isosbestic points indicated two binding modes. The first one may be due to intercalation, which is driven mainly by an electrostatic force between DNA and Eb and also the contribution of the hydrophobic environment between the base pairs. The second isosbestic point, which indicates the second binding mode, is attributed to outside binding driven by Coulombic interaction associated with an external site. This second point is found neither by the spectrophotometry technique nor by the fluorescence technique.

To analyze the Eb binding process to DNA by PAS it is necessary to consider the existence of two ways of decay for the molecule to return to the ground state, namely radiative and nonradiative decays. The PA amplitude signal depends directly on the conversion of the energy absorbed by the sample into heat. That is the reason why the PA lineshape spectrum is similar to that obtained by absorption.

The detection of the second isosbestic point by the absorption technique is not found in the literature and must be a consequence of signal saturation and practical difficulties, whereas the fluorescence amplitude signal for the intercalated binding mode is strong enough to hide the signal originating from the outside binding. However, with the PA technique, this fact helps to identify the second binding mode, which we consider to be associated with the second isosbestic point.

Using the theoretical model of McGhee-von Hippel (Eq. 3) that expresses the fitted parameters only in terms of ligand binding, which does not depend on any specific site of the DNA (McGhee and von Hippel 1974), and fitting the experimental data of the PA amplitude measurement of the DNA-Eb interaction, we obtained the values of K and n. The binding constant K was $3.40 \pm 0.02 \times 10^8\ M(bp)^{-1}$ and n was 2.03 ± 0.01. Owing to the existence of two isosbestic points, representing two binding modes, the binding constant here obtained must be adjusted, because its value is a composition of these two means of binding which are present in the concentration of Eb bound to DNA. To determine the exact concentration that saturates the primary rectangular hyperbola by plotting α_d versus SDS concentration site, we carried out experiments involving drug dissociation from DNA.

The method employed to induce DNA-dye dissociation was performed by incorporating the detergent SDS into the DNA-Eb complex. The SDS titration varied from 0 to 30.98 mM, as shown in Fig. 2. A small variation of 5 nm is observed and also an increment of the PA amplitude signal. At 21.48 mM of SDS titration, the PA amplitude signal was unchanged, indicating the maximum of Eb removed from the DNA. PAS measurement with SDS over the critical micellar concentration (cmc) did not affect the signal, which often happens with other techniques. The increment on the PA amplitude signal with SDS titration may be understood to be due to changes in the Eb photophysical properties. When Eb binds to DNA its fluorescent signal intensity increases (Waring 1965; LePecq and Paoletti 1967), reducing its nonradiative decay efficiency, which may be observed in Fig. 1, and when the Eb is dissociated from the DNA it recovers almost all of its nonradiative decay efficiency, and the PA amplitude signal increases, as shown in Fig. 2. Nevertheless, the PA amplitude signal increment, shown in Fig. 2, does not return to the initial value, indicating that not all the Eb is dissociated from the DNA. So we have evidence of strong and weak binding modes, respectively.

To confirm that the SDS captures the Eb weakly bound to the DNA while not removing the intercalated Eb, a titration with SDS to the Eb without DNA was performed with PAS (Fig. 3) under the same conditions. The results show that, below the cmc of SDS, the Eb amplitude decreases relative to that in solution. This presumably happens because of the formation of an associated complex involving the Eb cation and SDS anion, with the precipitation of the complex. Above the cmc of SDS [$\sim$1 mM in 150 mM ionic strength (Hunter 1992)], the amplitude gradually increases, indicating an increment of Eb solubilization in the solution. The

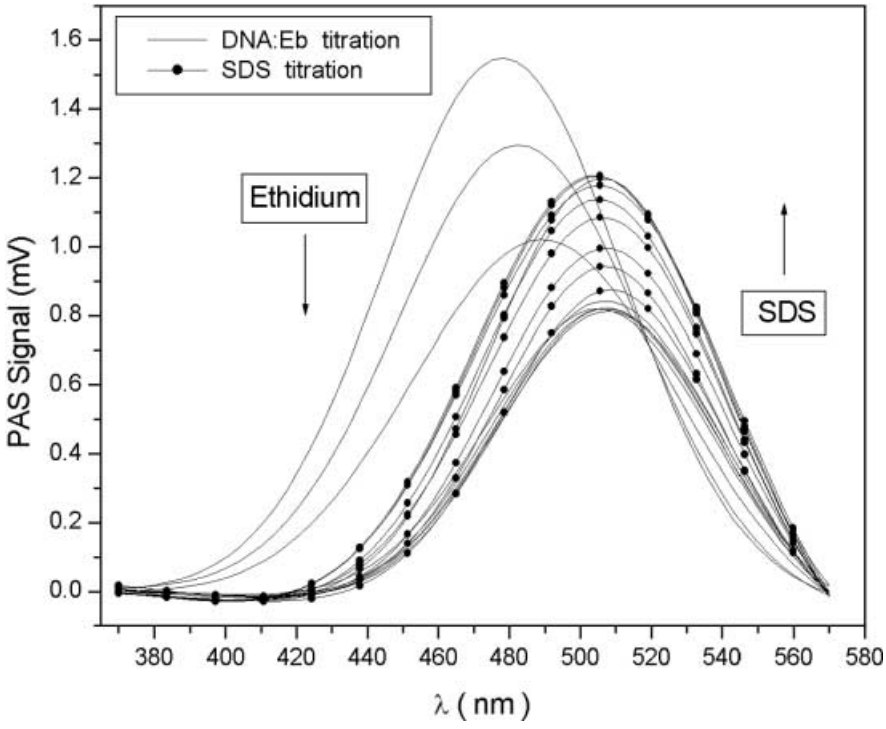

Fig. 2 Photoacoustic spectra of the SDS titration on the DNA-Eb complex, varying from 0 to 30.98 mM SDS with the DNA:Eb molar ratio at 5.53 and at 150 mM NaBr. The DNA-Eb complex was the same as that used in Fig. 1

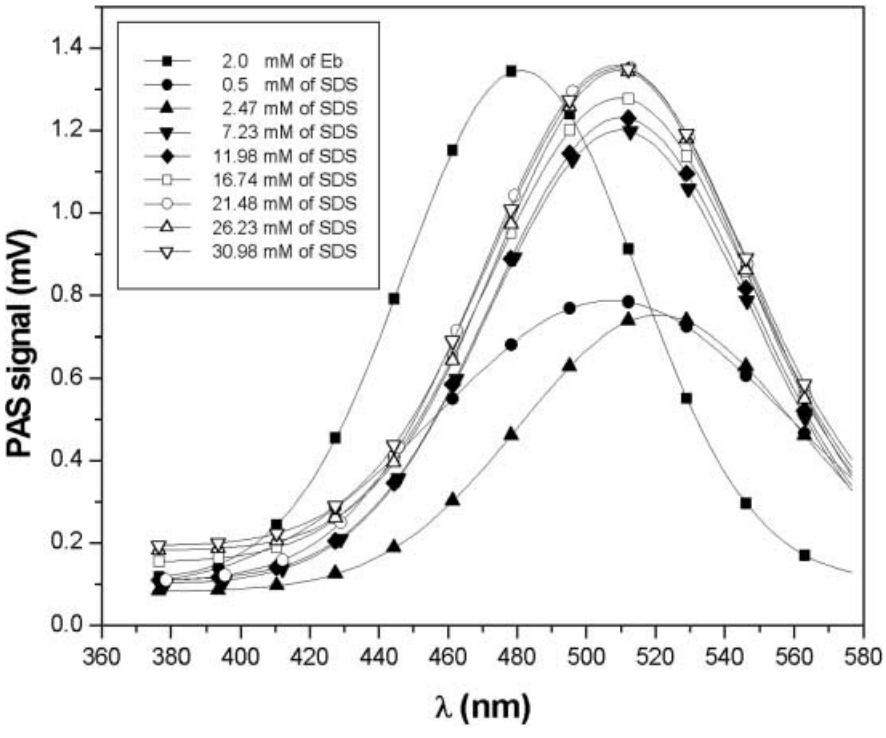

Fig. 3 Photoacoustic spectra of SDS titration on Eb, varying from 0 to 30.98 mM SDS at 150 mM NaBr

SDS-Eb complex amplitude reaches its maximum value, which is equal to that of free Eb in solution, indicating that all disposable Eb in the solution was strongly bound to the micelle. The amplitude also exhibits a distinct red shift from 480 nm to 508 nm. These results are in good agreement with the data obtained by absorption and fluorescence (Pal et al. 1998).

In our experiment we noted that, during the phase of precipitation, the precipitate complex deposited at the bottom of the sample holder did not contribute to the PA amplitude signal. This was because the effective optical absorption length of the sample is related to the amount of noncomplexed Eb, which is low in the precipitation process. This means that the concentration of

disposable Eb in the solution that produces the PA amplitude signal decreases relative to the initial concentration. On the other hand, with the addition of SDS, the PA amplitude signal recovers its initial value, as a clear effect of solubilization.

The Eb interacts with two distinct environments, DNA and SDS, so we can investigate the relationship between the photophysical properties of Eb and the microenvironment of each interaction. This is possible by observing both radiative and nonradiative decay yields. The Eb cation molecule is composed of two rings, a main phenanthridinium ring and a secondary phenyl ring. When Eb intercalates with DNA it is known that it uses the phenanthridinium ring. This intercalation increases the fluorescence intensity by 19 times that present in solution. While interacting with SDS it may use the phenyl ring, which increases the fluorescence intensity by 5.2 times that found in solution (Fig. 4). These results reinforce the observation that the Eb weakly bound to DNA is removed by the SDS titration and interacts with the micellar environment, inducing an increment of fluorescence intensity, although lower than when intercalated. That is the reason why the PA amplitude signal (Fig. 2) increases with the SDS titration, but not returning to the initial amplitude due to the fact that the population of removed Eb is smaller than the population of intercalated Eb.

The dissociation constant is obtained by applying a rectangular hyperbola adjustment to the plot of the fraction of removed Eb (α_d) against varying SDS concentration, from 0 to 21.48 mM of SDS titration. The adjustment of the experimental data and the theoretical rectangular hyperbola equation resulted in a correlation coefficient of 0.996 for eight points and the amount of Eb removed was 0.43 ± 0.04 mM. We noted that, at 2 mM SDS, 50% of Eb weakly bound to DNA is removed. The value of the dissociation constant, compared with the whole Eb concentration of 2 mM disposable in the solution, indicates that $21.5 \pm 2\%$ of this total binds externally to DNA, which is in full agreement with the literature which records a value of 20% (Nordmeier 1992).

The association and dissociation constants, when employed in the same equilibrium reaction, are expected to have reciprocal values. In the case where two binding modes are present, the inverse of the binding constant is different from the dissociation one. That is exactly what happens here, demonstrating a strong indication of the two Eb binding modes. Using the McGhee-von Hippel analysis we first applied it considering one binding mode, assuming it to be intercalation. With the new results obtained from the SDS titration, the quantity of Eb removed was lower than the total, denoting strong and weak binding modes, comparatively. The concentration of Eb intercalated with DNA used previously was adjusted by subtracting 0.43 mM from the total of 2 mM of Eb, and the McGhee-von Hippel analysis was employed again. Figure 5 shows the new normalized analysis, and the binding constant obtained for K was $1.20 \pm 0.01 \times 10^9$ M(bp)$^{-1}$ and n was 2.60 ± 0.03. The inset of Fig. 5 shows the amplitude of the intermediate titration positions. The practical difficulties associated with the titration are indicated by the error bars. The number of excluded sites increases from 2 to 2.6 for the adjusted data, implying a longer anticooperativity effect. This is consistent with our previous measurements in which,

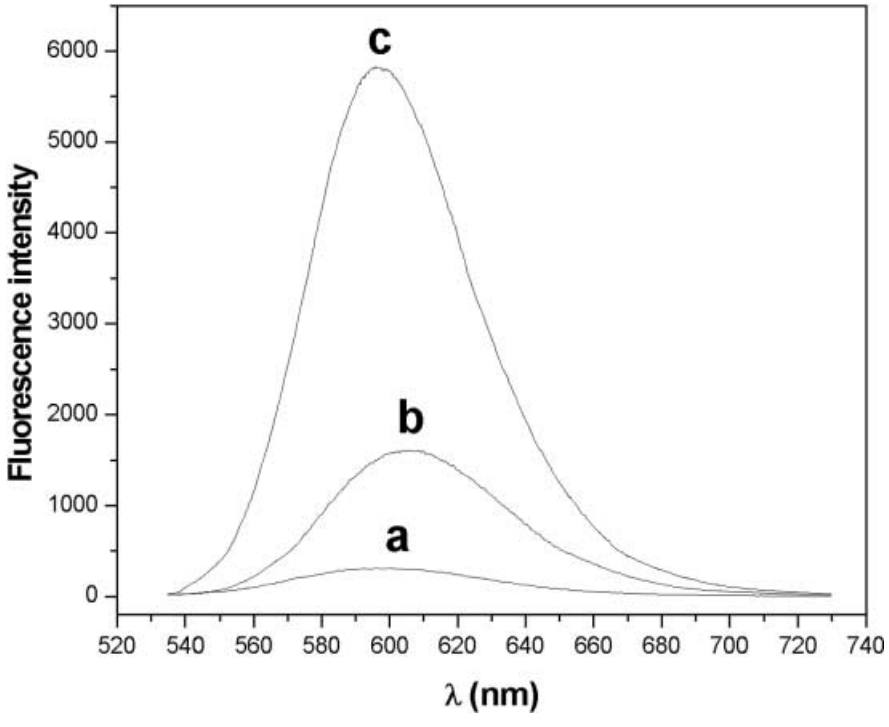

Fig. 4 Fluorescence maximum emission spectra of Eb in water at 150 mM NaBr in (*a*) 50 μM Eb, (*b*) 50 μM Eb in 2.62 mM SDS, and (*c*) 50 μM Eb intercalated with DNA

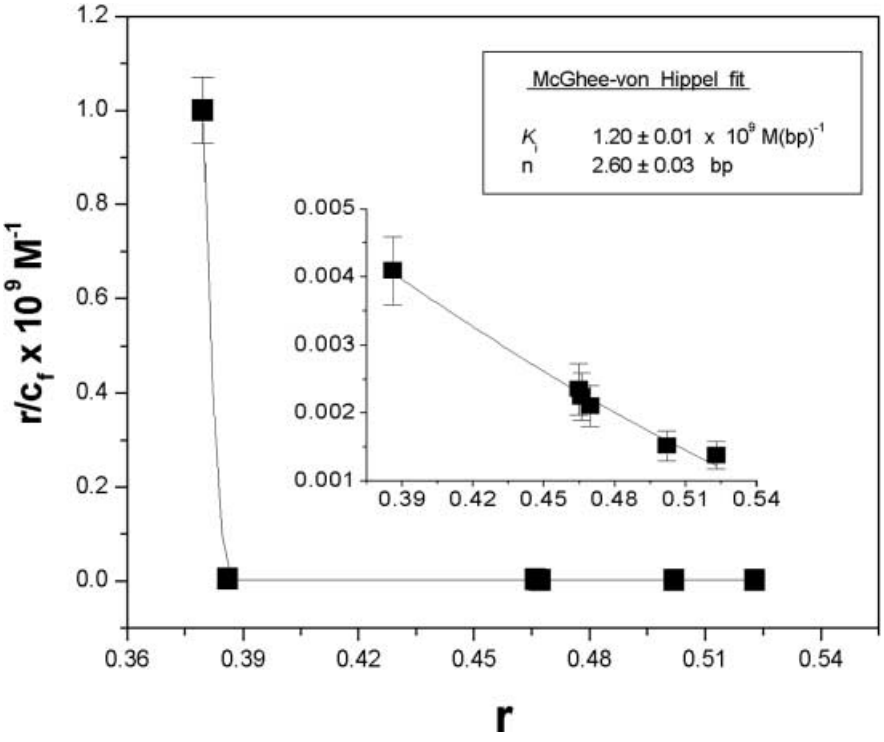

Fig. 5 Analysis of photoacoustic data at 480 nm for binding of ethidium bromide to calf thymus DNA. Data are plotted as r/C_f versus r at each titration point. Nonlinear fitting to the McGhee-von Hippel excluded-side model for $0.001 \leq \alpha \leq 0.999$ data gives the curve shown

during intercalation, the fluorescence lifetime of Eb increased from 1.65 ns in aqueous solution to 21 ns in DNA, and when the DNA:Eb molar ratio was between 2.5 and 3 the free Eb population disappeared (Bugs and Cornélio 2001). Our data therefore indicate that one Eb molecule excludes approximately three base pairs on intercalation, and during this complex-forming process the DNA elongation is accompanied by a local unwinding of the bases and a change in the sugar puckering.

The binding constant obtained here is somewhat higher than other reported values in the literature, which vary from 10^4 to 10^6 (LePecq and Paoletti 1967; McMurray and van Holde 1991; Nordmeier 1992; Das et al. 1999). On the other hand, we found in the literature highly DNA-affinic ligands whose binding constant values are in the 10^8–10^{10} M^{-1} range (Loontiens et al. 1990; Haq et al. 1995; Jenkins 1997). These differences show the complexity of the interaction between ligands and DNA, and the need for new methodologies to contribute to our understanding of this interaction. Owing to its complexity, analysis of this data was performed using a nonlinear equation for the neighbor exclusion model developed by McGhee and von Hippel. Jenkins (1997) reports that the binding data should initially be fitted for a practical $0.01 \leq \alpha \leq 0.99$ range, while for $0.001 \leq \alpha \leq 0.999$ a wider range of data should be introduced with caution because of the significant errors involved. In our analysis these two conditions were explored. The former resulted in moderate binding with a constant value of 10^6 M^{-1} and the latter around 10^9 M^{-1}. With the identification of the second isosbestic point, which is a strong indication of saturating the first binding mode, the error sources were reduced, and we used $0.001 \leq \alpha \leq 0.999$ in the analysis. The free binding energies may be calculated from this binding constant by using the standard relation $\Delta G^{\circ} = -RT \ln K$, yielding the value $\Delta G^{\circ} = -12.38$ kcal mol^{-1}.

According to the results presented, the accuracy of PAS is sufficient to detect two binding modes of Eb to DNA (Bugs 2001). It is also implicit that there are two distinct quantum efficiency yields of nonradiative decay as well as two distinct fluorescence efficiency quantum yields. As PA and fluorescence detect nonradiative decay and radiative decay, respectively, and assuming that Eb returns to its ground state using only nonradiative and radiative decays, it is possible to determine the quantum yield of Eb using PAS. The quantum yield was determined by comparing the integrated area under the curves shown in Fig. 1. Using free Eb as a standard sample, the quantum yield calculated as due to intercalation was 0.87 ± 0.01, which is in agreement with the figure in the literature of 0.90 (Cantor and Schimmel 1980; Pal et al. 1998). The second binding mode for Eb occurred when all the sites available for intercalation with the DNA were occupied. Then the Eb binds externally to DNA (most likely along the phosphate backbone). Calculating the quantum yield of this new condition, we obtained a value of 0.04 ± 0.01. The fall of the quantum yield elucidates the reason, because the fluorescence technique does not distinguish between these two binding modes, since the fluorescence signal of intercalated Eb is higher than Eb externally bound to DNA, thus masking its contribution. This result also confirms the existence of the second isosbestic point, because the reduction of the fluorescence quantum yield implies the accretion of the nonradiative yield, which

becomes detectable and represents the contribution of heat produced by Eb bound externally to DNA.

In conclusion, we have obtained new and interesting results with the employment of PAS investigating the interaction of Eb with DNA, demonstrating its capacity for determining two distinct binding modes of Eb to DNA which are usually only detectable by the combination of two or three techniques. The main advantage of this method is that a quantum yield for both binding modes can be obtained. The weak binding mode is associated with a low quantum yield, presumably because the ligand is exposed to solvent. Besides that, the dependency of the quantum yield upon these binding modes reinforces our finding that the value found for the binding constant is correct. As the first application of PAS investigating this interaction, it is shown to be capable of substituting conventional spectroscopies, and the results may be used to throw light upon the association process between Eb and DNA. Finally, the perspective of applying PAS to the investigation of nonfluorescence and low quantum yield drugs, while interacting with DNA or proteins, is very promising.

Acknowledgements This work was supported by Fundação de Amparo a Pesquisa do Estado de São Paulo (FAPESP) (grant no. 95/5038-6). M.R.B. is recipient of a FAPESP fellowship (grant no. 96/07843-6).

References

Abbruzzetti S, Crema E, Masino L, Vecli A, Viappiani C, Small JR, Libertini LJ, Small EW (2000) Fast events in protein folding: structural volume changes accompanying the early events in the N→I transition of apomyoglobin induced by ultrafast pH jump. Biophys J 78:405–415

Adams MJ, Highfield JG, Kirkbright GF (1977) Determination of absolute fluorescence quantum efficiency of quinine bisulfate in aqueous medium by optoacoustic spectrometry. Anal Chem 49:1850–1852

Adams MJ, Highfield JG, Kirkbright GF (1980) Determination of the absolute quantum efficiency of luminescence of solid materials employing photoacoustic spectroscopy. Anal Chem 52:1260–1264

Bresloff JL, Crothers DM (1981) Equilibrium studies of ethidium-polynucleotide interactions. Biochemistry 20:3547–3553

Bugs MR (2001) Monitoramento de propriedades fotofísicas e fisico-químicas da interação do brometo de etídio ao DNA por fotoacústica, fluorescência e FTIR. PhD thesis, Physics Department, IBILCE, UNESP, Brazil

Bugs MR, Cornélio ML (2001) Analysis of the ethidium bromide bound to DNA by photoacoustic and FTIR spectroscopy. Photochem Photobiol 74:512–520

Burns VWF (1969) Fluorescence decay time characteristics of the complex between ethidium bromide and nucleic acids. Arch Biochem Biophys 133:420–424

Byrne CD, Mello AJ de (1998) Photophysics of ethidium bromide complexed to ct-DNA: a maximum entropy study. Biophys Chem 10:173–184

Cantor CR, Schimmel PR (1980) Biophysical chemistry, part II: techniques for the study of biological structure and function. Freeman, San Francisco, pp 445–446

Cornélio ML, Sanches R (1994) The use of photoacoustic spectroscopy to determine the critical distance for electron transfer. J Biochem Biophys Methods 29:149–155

Cornélio ML, Sanches R (1995) Monitoring electron transfer by photoacoustic spectroscopy. Eur Biophys J 23:439–442

Das S, Kumar GS, Maiti M (1999) Conversions of the left-handed form and the protonated form of DNA back to the bound right-handed form by sanguinarine and ethidium: a comparative study. Biophys Chem 76:199–218

Douthart RJ, Burnett JP, Beasley FW, Frank BH (1973) Binding of ethidium bromide to double-stranded ribonucleic acid. Biochemistry 12:214–220

Fork DC, Herbert SK (1993) The application of photoacoustic techniques to studies of photosynthesis. Photochem Photobiol 57:207–220

Haq I, Lincoln P, Suh D, Norden B, Chowdhry BZ, Chaires JB (1995) Interaction of Δ- and Λ-$[Ru(phen)_2DPPZ]^{2+}$ with DNA: a calorimetric and equilibrium binding study. J Am Chem Soc 117:4788–4796

Heller DP, Greenstock CL (1994) Fluorescence lifetime analysis of DNA intercalated ethidium bromide and quenching by free dye. Biophys Chem 50:305–312

Holde KE van, Johnson WC, Ho PS (1998) Principles of physical biochemistry. Prentice Hall, Englewood Cliffs, NJ, pp 587–638

Hunter RJ (1992) Foundations of colloid science, vol. 1. Clarendon Press, Oxford, pp 564–625

Jenkins T (1997) Optical absorbance and fluorescence techniques for measuring DNA-drug interactions. In: Fox KR (ed) Drug-DNA interactions protocols. Humana Press, Totowa, NJ, pp 195–218

Kurian E, Prendergast FG, Small JR (1997) Photoacoustic analysis of proteins: volumetric signals and fluorescence quantum yields. Biophys J 73:466–476

Lahmann W, Ludewig HJ (1977) Opto-acoustic determination of absolute quantum yields in fluorescent solutions. Chem Phys Lett 45:177–179

LePecq J-B, Paoletti C (1967) A fluorescent complex between ethidium bromide and nucleic acid: physical-chemical characterization. J Mol Biol 27:87–106

Lerman LS (1961) Structural considerations in the interaction of DNA and acridines. J Mol Biol 3:18–30

Li HJ, Crothers DM (1969) Relaxation studies of the proflavine-DNA complex: the kinetics of an intercalation reaction. J Mol Biol 39:461–477

Loontiens FG, Regenfuss P, Zechel A, Dumortier L, Clegg RM (1990) Binding characteristics of Hoechst 33258 with calf thymus DNA, poly[d(A-T)], and d(CCGGAATTCCGG): multiple stoichiometries and determination of tight binding with a wide spectrum of site affinities. Biochemistry 29:9029–9039

Malkin S, Cahen D (1979) Photoacoustic spectroscopy and radiant energy conversion: theory of the effect with special emphasis on photosynthesis. Photochem Photobiol 29:803–813

Mandelis A (1982) Photoacoustic determination of the non-radiative quantum efficiency of uranyl formate monohydrate, $UO_2(HCOO)_2.H_2O$, powders. Chem Phys Lett 91:501–505

McCann J, Spingarn NE, Kobori J, Ames BN (1975) Detection of carcinogens as mutagens: bacterial tester strains with R factor plasmids. Proc Natl Acad Sci USA 72:979–983

McGhee JD, Hippel PH von (1974) Theoretical aspects of DNA-protein interactions: co-operative and non-co-operative binding of large ligands to a one-dimensional homogeneous lattice. J Mol Biol 86:469–489

McMurray CT, Holde KE van (1991) Binding of ethidium to the nucleosome core particle. 1. Binding and dissociation reactions. Biochemistry 30:5631–5643

Nordmeier E (1992) Absorption spectroscopy and dynamic and static light-scattering studies of ethidium bromide binding to calf thymus DNA: implications for outside binding and intercalation. J Phys Chem 96:6045–6055

Pal SK, Mandal D, Bhattacharyya K (1998) Photophysical processes of ethidium bromide in micelles and reverse micelles. J Phys Chem B 102:11017–11023

Perkampus H-H (1992) Recent developments in UV-vis spectroscopy. In: Perkampus H-H (ed) UV-vis spectroscopy and its

applications. Springer, Berlin Heidelberg New York, pp 101–120
Quimby RS, Yen WM (1980) Photoacoustic measurement of the ruby quantum efficiency. J Appl Phys 51:1780–1872
Rosencwaig A (1980) Photoacoustics and photoacoustics spectroscopy. Wiley, New York
Suh D, Chaires JB (1995) Criteria for the mode of binding of DNA binding agents. Bioorg Med Chem 3:723–728
Tsai C-C, Jain SC, Sobell HM (1977) Visualization of drug-nucleic acid at atomic resolution. I. Structure of an ethidium/dinucleoside monophosphate crystalline complex, ethidium 5-iododouridylyl (3′-5′) adenosine. J Mol Biol 114:301–315
Waring MJ (1965) Complex formation between ethidium bromide and nucleic acids. J Mol Biol 13:269–282
Waring MJ (1981) DNA modification and cancer. Annu Rev Biochem 50:159–192
Yguerabide J, Ceballos A (1995) Quantitative fluorescence method for continuous measurement of DNA hybridization kinetics using a fluorescent intercalator. Anal Biochem 228:208–220